Open access • Journal Article • DOI:10.1109/77.828235

Mechanical design and analysis of the Fermilab 11 T Nb/sub 3/Sn dipole model

Giorgio Ambrosio, N. Andreev, D.R. Chichili, Iouri Terechkine ...+4 more authors

Institutions: Fermilab, KEK

Published on: 26 Jan 2000 - IEEE Transactions on Applied Superconductivity (IEEE)

Topics: Electromagnetic coil, Magnet, Superconducting magnet, Very Large Hadron Collider and Niobium-tin

Fermi National Accelerator Laboratory

FERMILAB-Conf-99/371

Mechanical Design and Analysis of the Fermilab 11 T Nb_3Sn Dipole Model

G. Ambrosio et al.

Fermi National Accelerator Laboratory
P.O. Box 500, Batavia, Illinois 60510

January 2000

Presented at and to Appear in the Published Proceedings of the *16th International Conference on Magnet Technology*, Ponte Vedra Beach, Florida, September 26-October 2, 1999

Operated by Universities Research Association Inc. under Contract No. DE-AC02-76CH03000 with the United States Department of Energy

Mechanical Design and Analysis of the Fermilab 11 T Nb_3Sn Dipole Model

G. Ambrosio, N. Andreev, D.R. Chichili, I. Terechkine, S. Yadav, A.V. Zlobin
FNAL, Batavia, IL, USA

S. Caspi
LBNL, Berkeley, CA, USA

M. Wake
KEK, Japan

Abstract—The goal of the Fermilab High Field Magnet (HFM) R&D project is to explore various designs and production technology of a high-field, low-cost Nb_3Sn accelerator magnet suitable for a future Very Large Hadron Collider (VLHC). The model under fabrication consists of two-layer shell-type coil with 43.5 mm aperture and cold iron yoke. Fermilab concept of magnet design and fabrication technology involves some specific features such as curing of half-coil with ceramic binder/matrix before reaction, and then simultaneous reaction and impregnation of both half-coils to get a "coil pipe" structure. The coil pipe is mechanically supported by the vertically-split iron yoke locked by two aluminum clamps and a thick stainless steel skin. 2D finite element analysis has been performed to study and optimize the prestress in the coil and in the structural elements at room temperature and at 4.2 K. Model description, material properties and the results of mechanical analysis are reported in this paper.

I. Introduction

The long term goal of the Fermilab HFM program is to develop a high field, low cost superconducting magnet for use in future VLHC. The short term objective, however, is to explore various designs and fabrication technology to built and test 10-11 T accelerator type dipole magnets, operating at 4.2 K with both wind and react [1] and react and wind technology [2]. The first model being fabricated is based on a two layer cosθ coil structure with wind and react technology and a cold iron yoke [1].

The high sensitivity of Nb_3Sn cable to strain makes the coil mechanical stability a key issue for the high field magnets. The required prestress is determined by the magnet design, the operating field and the thermo-mechanical properties of the coil as well as the magnet structural materials. The prestress applied to the magnet at room temperature must be sufficient to compensate for the stress reduction due by coil creep, differential thermal contraction during cool down and Lorentz forces during magnet excitation. However, the pre-stress should be low enough not to cause degradation of cable critical current.

Finite element analysis using ANSYS has been performed to optimize the coil prestress and to minimize the stress in the major elements of the coil support structure. The goal is to develop a robust mechanical design, which is flexible to account for changes in prestress due to manufacturing uncertainties and tolerances. This paper reports the main results of this analysis.

Manuscript received September 27, 1999.
Work is supported by the U.S. Department of Energy.

II. Magnet Design

The model is a 43.5 mm bore, 1 m long dipole magnet with a two-layer cosθ Nb_3Sn coil. The magnet cold mass cross-section is shown in Fig. 1. The coils are made of Rutherford type Nb_3Sn cable with 28 strands, 1 mm in diameter insulated with a ceramic tape. Each half-coil consists of 24 turns, 11 turns in the inner layer and 13 turns in the outer layer. Four spacers per quadrant, two for each layer, are used to minimize the lower order geometrical harmonics and to ensure the radial turn position in the coil. In the present design, the two pole posts, one in the inner half-coil and the another in the outer half-coil, are part of the coil. A vertical cut was introduced in the inner pole posts to reduce the pole stiffness thus decreasing the pre-stress in the coil.

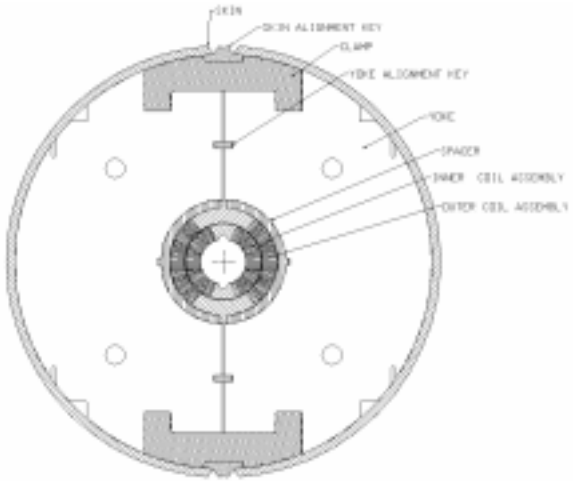

Fig. 1. Cross section of the first dipole model.

The coils are mechanically supported by the vertically split iron yoke which in turn is supported by two clamps and a stainless steel skin. Thick end plates are used to restrict the longitudinal coil motion under Lorentz forces. Two 8 mm thick spacers fill the space between the coil and the yoke and are designed to protect the coil during assembly. The coils are centered with respect to the spacers by two vertical pole extensions while the spacers will be centered with respect to the yoke by two keys on the mid-plane. The spacer/pole extension interference will ensure contact between the two at all stages of the magnet.

The initial pre-stress of the coil during assembly and the control of magnet geometry (vertical gap) at room temperature is provided by two clamps. The final prestress at operating temperature and field necessary to avoid the radial and azimuthal turn motion under Lorentz forces is obtained using a two-piece iron yoke, clamps and a welded stainless steel skin. The key features of this mechanical design come from the simultaneous reaction and impregnation of both coils to produce the "coil pipe" [3]. This eliminates the problem of shimming the mid-plane to get a planar surface and allows using thin spacers between coils and yoke instead of collars. The required prestress is therefore applied radially through the spacers and the yoke by the skin and the clamps.

III. Analysis

A. Model Description

A finite element model has been created to analyze the mechanical design. Fig. 2 shows the $ANSYS_{5.5}$ model used for the analysis presented in this paper.

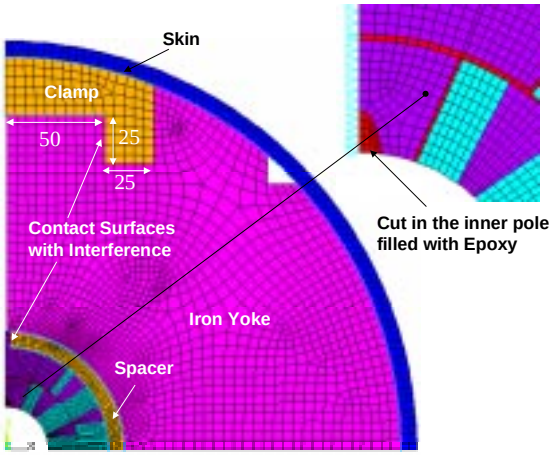

Fig. 2. ANSYS model for stress analysis.

Quarter symmetry is used to reduce the model size (4100 elements) and solution time. The coils and the pole are glued to form the "coil pipe". Since many contact surfaces are involved in the model, different contact elements were studied and then compared with an analytical model to choose the best contact elements and their properties [4]. Frictional (μ=0.07) contact elements (CONTAC 48) were used between the inner radius of the spacer and the outer ground insulation, between the outer radius of the spacer and the inner radius of the yoke and between the outer radius of the yoke and the skin. The azimuthal interference between the spacer and the pole extension (0.1 mm) and the interference between the clamp and the yoke (0.3 mm) were obtained through COMBIN40 elements. The weld shrinkage was modeled by applying a displacement to the skin at room temperature (0.4 mm) [5].

In order to compute the magnetic forces on the coils a finite element analysis of the cross section with a finite iron permeability of μ_r=1000 (to be conservative) was performed using ANSYS. Additional characteristics of the model are:

- A shell section represents each coil block. The sides of each shell section are two straight lines and two arcs centered in the aperture center. The edges of each bare block computed by ROXIE [6] were used to obtain the edges of these shell blocks.
- Each coil block has a uniform current distribution. The value of the current density in each block was computed to have the right overall current (i.e. the current in each cable times the number of cables in that block).
- A quadratic mesh was used in all coil blocks and wedges. Inside each inner layer block the number of elements in azimuthal direction is equal to the number of cables.
- Layer to layer and ground insulation was modeled separately from the coil layers.

Fig. 3 shows the Lorentz force distribution in the cross-section at the maximum field. The resulting forces were compared with ROXIE and showed a very good agreement ($\Delta F/F < 1\%$). The Cartesian and Polar components of the forces at the nominal field, 11 T are: F_x = 2.8 MN/m, F_y = -1.1 MN/m and F_r = 1.6 MN/m, F_θ = -2.3 MN/m.

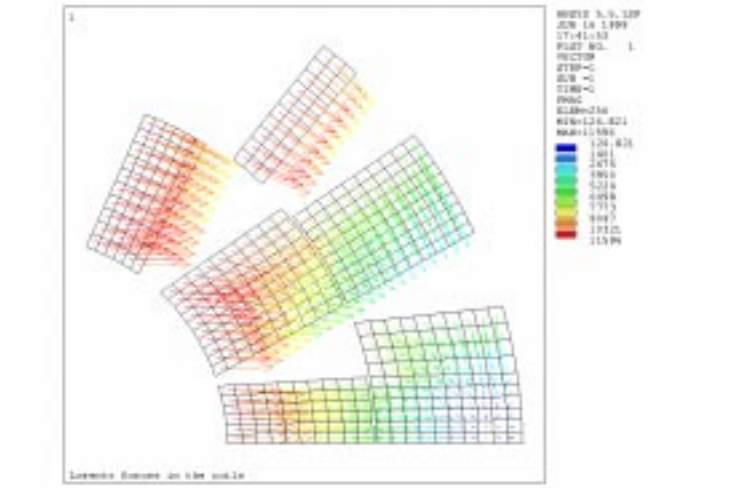

Fig. 3. Lorentz forces in the cross-section.

B. Material Properties

Table I lists the thermal and mechanical properties of the different materials used in the model.

TABLE I
THERMO-MECHANICAL PROPERTIES OF MATERIALS

Material	E_{300} GPa	$E_{4.2}$ GPa	ν	Therm.Cont K^{-1} (x 10^{-5})
Coil – azimuthal	38	38	0.33	1.21
Coil – radial	44	55	0.33	0.90
G10 – insulation	14	14	0.3	2.58
Copper (pole)	120	150	0.3	1.128
Aluminum	70	81.6	0.3	1.47
Iron	210	225	0.3	0.70
Stainless Steel	210	225	0.3	1.027

Orthotropic properties in cylindrical coordinates have been used for the coil. Mechanical properties (E, α, ν) of the coil measured using ten-stack samples after reaction and

impregnation have shown a non-linear behavior during the first loading cycle and a linear behavior with higher stiffness for the successive loading cycles. These effects are observed both at room temperature and at 4.2 K [7]. Data presented in Table I corresponds to the linear behavior achieved after saturating load cycles (massaging).

C. Results

Several cases including open or closed yoke gap, different materials for clamps and coil/yoke spacers, use of clamps and/or skin welding under pressure, etc. have been studied. The analysis has been carried out for the following stages: (a) the insertion of the clamps and skin welding at room temperature; (b) at 4.2 K without Lorentz forces; and at 4.2 K (c) at nominal [11 T] and (d) at maximum [12 T] field. The following conditions were considered in the analysis:

- During the magnet assembly the coils will be repetitively loaded and unloaded (massaged) to obtain a linear behavior and higher stiffness for successive loading - unloading cycles [7].
- Clamps will be inserted after massaging giving some moderate prestress to the coils. Tapered surfaces will be used to reduce the spring back. The final pre-stress will be provided by welding the skin onto the yoke under pressure.
- During cool down the skin and the clamps contract more than the yoke increasing the prestress in the coils. Spacers will be in contact with the yoke at all stages of the magnet.
- During excitation, azimuthal Lorentz forces decrease the coil pre-stress at the pole region, however the coil remains in contact with the pole.

The criteria for an acceptable solution are:

- the peak stress in the coils should be less than 125 MPa
- all parts of the coils should be in compression at nominal operation field.

Additional parameters are coil deformation and shear stress. The results of the analysis are summarized in Table II. It was found that all cases provided reliable mechanical stability to the coil structure except the last cases without skin participation as mechanical structural element.

TABLE II
MECHANICAL DESIGNS STUDIED

Skin	Clamp	Yoke gap	Clamp Material	Spacer Material	Result
Yes	Clamp	Open	Al	Al	OK
Yes	Clamp	Open	St. steel	Al	OK
Yes	Clamp	Open	St. steel	St. steel	OK
Yes	No	Open	Al	St. steel	OK
Yes	No	Closed	Al	St. steel	OK
No	Clamp	Open	Al	Al	NO
No	Clamp	Open	St. steel	St. steel	NO
No	Clamp	Open	bronze	bronze	NO

The first case reported in Table II is chosen as a base-line for the first short model and its analysis is reported in detail here. Fig. 4, 5 and 6 show the azimuthal stress distribution in the coil at room temperature, 4.2 K without current and at nominal current (11T) respectively. Coils in each model have the same mesh as in the magnetic model to allow the automatic loading of the magnetic forces.

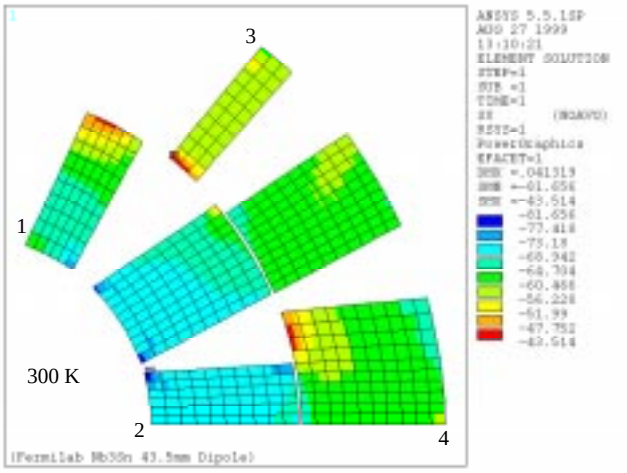

Fig. 4. Azimuthal stress in the coil at 300 K after assembling.

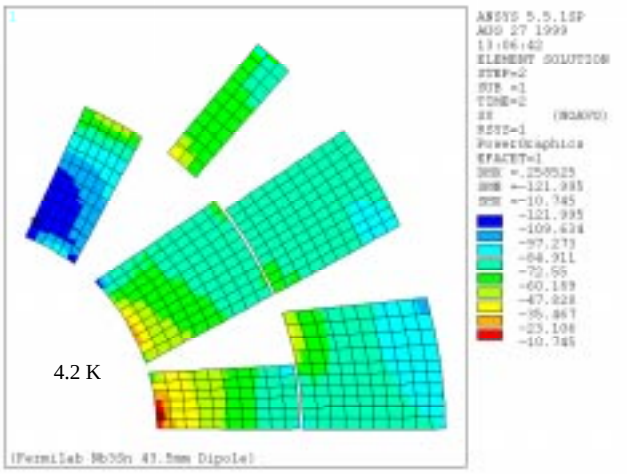

Fig. 5. Azimuthal stress in the coil after cool down.

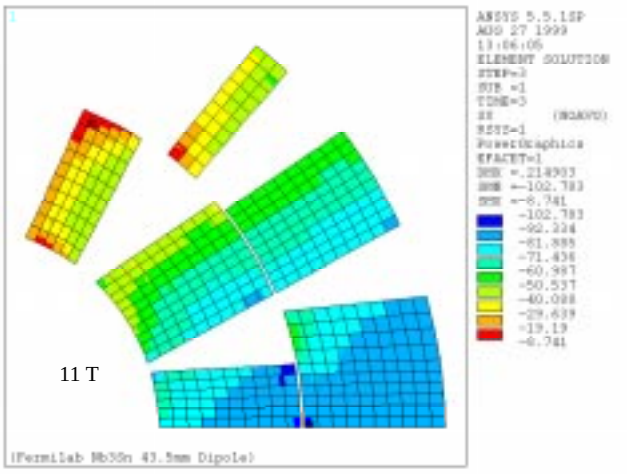

Fig. 6. Azimuthal stress in the coil at 11 T.

At room temperature after clamp insertion and skin welding, a maximum stress of 82 MPa is seen at the inner-layer inner radius near the wedge (Fig. 4). Local minimum is

due to the wedge being stiffer than the coil. Clamps provide about 40% of the total prestress at room temperature. The coil bore is almost circular with a difference of about 4 μm between horizontal and vertical radii.

After cool down the stress distribution on the inner radius is rather non-uniform due to the compression of the coil in the horizontal direction (Fig. 5). The difference between the coil inner radius on the horizontal plane and on the vertical plane reaches about 98 μm. The pre-stress ranges from 122 MPa in the inner-layer pole turn to 11 MPa near the inner-layer mid-plane turn. Note that the peak stress would be about 150 MPa without the cut in the pole.

At nominal field (Fig. 6) all parts of the coil are still under compression and the maximum stress of 103 MPa is at the inner and outer-layer mid-plane in a low field region. At 12 T the pattern is the same but few elements at the pole see small tension. The coil bore shape becomes again close to a circle with small difference of about 9 μm between horizontal and vertical radii.

Shear stresses on all major surfaces inside the coil and between the coil and support structure is less than 28 MPa at all conditions. A summary of the results is given in Tables III and IV which includes the azimuthal and radial stress at four points of the coil, and maximum equivalent stress in the coil and major elements of the mechanical structure after assembling, cool down, at nominal and at maximum field.

TABLE III
RADIAL AND AZIMUTHAL STRESS IN THE COIL
(SEE FIG. 4 FOR POSITIONS)

Coil position	300 K		4.2 K		11 T		12 T	
	σ_θ	σ_r	σ_θ	σ_r	σ_θ	σ_r	σ_θ	σ_r
1	69	2	122	0	9	0	-5	0
2	73	2	23	0	82	0	93	0
3	60	35	85	70	51	60	44	50
4	65	40	97	52	93	94	103	100

TABLE IV
PEAK EQUIVALENT STRESS (MPa) IN THE COIL AND MAJOR ELEMENTS OF MECHANICAL SUPPORT STRUCTURE

	300 K	4.2 K	11 T	12 T
Coil	80	121	100	104
Spacer	166	125	97	97
Yoke	110	110	133	133
Clamp	135	124	128	128
Skin	200	330	350	350

It can be seen from the above tables that the maximum stress in the coil is always less than 125 MPa and the maximum stress in the support structure is below the material yield stress at all conditions.

D. Sensitivity Analysis

The effect of variation in the dimensions of the major components of the mechanical design were analyzed [8]. Fig. 7 shows an example where the clamp/yoke interference was varied keeping the spacer/pole interference and the weld shrinkage constant. As the clamp/yoke interference increases, the pre-stress in the coils also increases. Acceptable interference range is when the stress in the coils is within the range 0-125 MPa. Table V summarizes the results from the sensitivity analysis. Note that the nominal values and their acceptable variations for the main elements of magnet mechanical structure are reasonable from the manufacturing viewpoint.

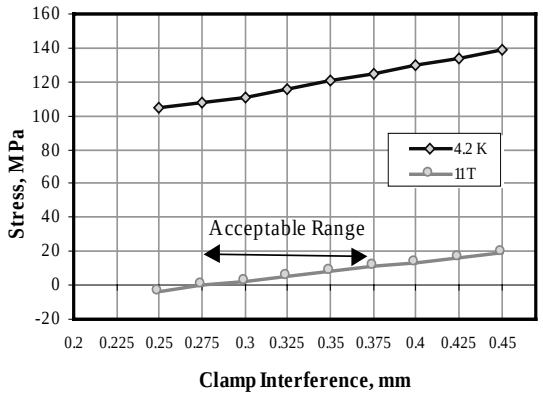

Fig. 7. Sensitivity analysis of clamp yoke interference.

TABLE V
SENSITIVITY ANALYSIS RESULTS

	Min	Max
Clamp/yoke interference	0.275	0.375
Spacer/pole interference	0.100	0.175
Deviat. of "coil pipe" OD	-0.025	+0.025
Weld shrinkage.	0.30	0.45

IV. CONCLUSIONS

A mechanical analysis shows that for the chosen magnet design and fabrication technology a sufficient radial and azimuthal coil prestress can be supplied by the yoke/skin structure. A maximum stress of 122 MPa is reached in the conductor after cool down near the inner pole region. This also leads to the non-uniform radial deformation of the coil assembly. However during excitation the coil returns to its circular shape with a maximum stress of about 103 MPa at the low field region. This will reduce any significant Ic degradation due to the transverse pressure. The impact of coil deformation on the field quality should be acceptable and is being studied.

REFERENCES

[1] G. Ambrosio et al. "Development of the 11 T Nb_3Sn Dipole Model at Fermilab", *MT-16*, Tallahassee, FL, 1999.

[2] G. Ambrosio et al. "Conceptual Design of a Block-Type Dipole for VLHC", *MT-16*, Tallahassee, FL, 1999.

[3] N. Andreev et al., "Fabrication and Testing of High Field Dipole Mechanical Model", ", *MT-16*, Tallahassee, FL, 1999.

[4] G. Ambrosio, "Mechanical design and analysis of a 40mm aperture high field Nb_3Sn dipole using skin welding to apply all prestress", Fermilab, TD-99-031, June 1999.

[5] D. R. Chichili, "Mechanical Analysis of the 44.5 mm bore Nb_3Sn Dipole Magnet", Fermilab, TD-99-030, April 1999.

[6] S. Russenchuck, "A Computer Program for the Design of Superconducting Accelerator Magnets", CERN AT/95-39, 1995.

[7] D. R. Chichili, et al.," Investigation of Cable Insulation and Thermo-Mechanical Properties of Nb_3Sn Composite", *MT-16*, Tallahassee, FL, 1999.

[8] D. R. Chichili et al. "Mechanical and Sensitivity Analysis of 43.5 mm bore Nb_3Sn Dipole Model", Fermilab, TD-99-035, July 1999.